Published in final edited form as:
Nanomedicine. 2013 January ; 9(1): 130–140. doi:10.1016/j.nano.2012.03.004.

Nanoliposomal minocycline for ocular drug delivery

James M. Kaiser, MS[a], **Hisanori Imai, MD**[b], **Jeremy K. Haakenson, BS**[a], **Robert M. Brucklacher, MS**[a], **Todd E. Fox, PhD**[a], **Sriram S. Shanmugavelandy, MS**[a], **Kellee A. Unrath, BS**[a], **Michelle M. Pedersen, BS**[a], **Pingqi Dai, MS**[a], **Willard M. Freeman, PhD**[a], **Sarah K. Bronson, PhD**[c], **Thomas W. Gardner, MD**[b,d], and **Mark Kester, PhD**[a,c,*]

[a]Department of Pharmacology, Pennsylvania State College of Medicine, Hummelstown, Pennsylvania, USA

[b]Department of Ophthalmology, Pennsylvania State College of Medicine, Hummelstown, Pennsylvania, USA

[c]Department of Cellular and Molecular Physiology, Pennsylvania State College of Medicine, Hummelstown, Pennsylvania, USA

[d]Department of Ophthalmology and Visual Sciences, University of Michigan, Ann Arbor, Michigan, USA

Abstract

Nanoliposomal technology is a promising drug delivery system that could be employed to improve the pharmacokinetic properties of clearance and distribution in ocular drug delivery to the retina. We developed a nanoscale version of an anionic, cholesterol-fusing liposome that can encapsulate therapeutic levels of minocycline capable of drug delivery. We demonstrate that size extrusion followed by size-exclusion chromatography can form a stable 80-nm liposome that encapsulates minocycline at a concentration of 450 ± 30 μM, which is 2% to 3% of loading material. More importantly, these nontoxic nanoliposomes can then deliver 40% of encapsulated minocycline to the retina after a subconjunctival injection in the STZ model of diabetes. Efficacy of therapeutic drug delivery was assessed via transcriptomic and proteomic biomarker panels. For both the free minocycline and encapsulated minocycline treatments, proinflammatory markers of diabetes were downregulated at both the messenger RNA and protein levels, validating the utility of biomarker panels for the assessment of ocular drug delivery vehicles.

Keywords

Minocycline; Diabetic retinopathy; Liposomes; Transcriptomics; Inflammation

Diabetic retinopathy (DR) is a progressive chronic disease that is the leading cause of preventable blindness among working-age adults within developed countries. Although many different types of drugs are currently being used offlabel for the treatment and prevention of diabetic retinopathy, there are no US Food and Drug Administration (FDA)–approved pharmacotherapies labeled for the prevention or treatment of DR specifically.[1] Because of the prevalence and debilitating effects of advanced DR, it is necessary to expand

*Corresponding author: Department of Pharmacology, Pennsylvania State College of Medicine, Hummelstown, Pennsylvania 17036, USA. mxk38@psu.edu (M. Kester).

Conflict of Interest Statement: Penn State Research Foundation has licensed several nanotechnologies, including nanoliposomes, to Keystone Nano, Inc. (State College, PA). M. Kester is the Chief Medical Officer of Keystone Nano, Inc.

on the current pharmacotherapeutic options, as well as to make advances toward novel pharmacological delivery approaches. Liposomes and other nanotechnologies have been used as delivery vehicles for therapeutic agents in ocular drug delivery, as they improve pharmacokinetic profiles and reduce toxicity.[2,3] The potential for these improved properties has spurred the scientific investigation of liposomal formulations of various drugs from nearly every topically or subconjunctivally administered ophthalmic drug class.[4] In general, local administration of liposomal-encapsulated drugs was found to significantly decrease the rate of clearance from the injection site and avert systemic toxicities.[2-4] Yet it has also been observed that these liposomal formulations can sometimes collect within and cloud the vitreous. Frequently, these various nanoscale formulations are heterogeneous in size and agglomerate to 500 nm or more. Thus, encapsulation of drugs within a stable nanoscale homogeneous formulation may have the potential to improve delivery of therapeutic doses.

The streptozotocin (STZ)-induced Sprague Dawley rat model of DR is known to phenotypically display an increased rate of neuronal apoptosis and an increase in retinal vascular permeability[5]—both hallmarks of human DR. Also, a highly reproducible panel of gene expression biomarkers has recently been described for the STZ-diabetic Sprague Dawley rat retina.[6,7] These transcriptional biomarkers of DR encode proteins linked to dysfunctional microvascular, neuronal, and inflammatory phenotypes associated with DR. In addition, a proteomic panel of diabetic-induced gene products that are not responsive to insulin treatment in a diabetic model has also recently been validated.[8] This study utilizes these biomarkers as surrogate end points to test the efficacy of a locally administered nanoscale therapeutic.

It is well established that molecular events underlying DR, like other pathological consequences of type I diabetic complications, are proinflammatory in nature.[5] Minocycline, an FDA-approved antibiotic, also has multiple anti-inflammatory modes of action in eukaryotic systems. Known eukaryotic molecular targets of minocycline are matrix metalloproteinase-9,[9,10] vascular endothelial growth factor A,[11] arachidonate 5-lipoxygenase,[12,13] cytochrome c,[14,15] interleukin-1β,[16,17] and caspase 1 and 3.[16,18] Systemic administration of minocycline has been shown to be efficacious in DR by reducing retinal proinflammatory cytokine expression, microglia activation, and caspase 3 activation in the STZ Sprague Dawley rat model.[19] However, as with most antibiotics, there are significant risks associated with long-term systemic administration. Local injections of minocycline in nanoliposomal form may afford the patient therapeutic benefit without needless exposure to high systemic minocycline serum levels that can potentially induce adverse reactions.[20-23] In this study, we explore the utility of nanoliposome-encapsulated minocycline as a subconjunctivally administered pharmacotherapy for DR.

Methods

Liposomal preparations

To prepare a minocycline-encapsulated nanoscale liposomal formulation, we substantially adapted previously described methods for encapsulation of tetracycline derivatives.[24-26] Chloroform-based stock solutions of egg phosphatidylcholine (Avanti Polar Lipids, Alabaster, Alabama), dihexadecyl phosphate and cholesterol (Sigma Aldrich, St Louis, Missouri) were mixed together in borosilicate glass test tubes at a molar ratio of 7:2:1. The solvent was completely removed via a constant flow of nitrogen gas at room temperature (21°–27°C). Liposomal formulations were hydrated with 800 μL of sterile isotonic 0.9% NaCl (v/v) hydration solution (Baxter Healthcare, Deerfield, Illinois) at 60°C and briefly vortexed every 10–15 minutes for 2 hours. Formulations were sonicated for 1 minute at 60°C, and then 200 μL of 100 mM minocycline, pH 7.2 (Sigma Aldrich) were added to the preparation and incubated with the liposomes for 30 minutes. The formulation was then

extruded 13 times through a 100-nm polycarbonate membrane utilizing an Avanti mini-extruder. Encapsulated minocycline was separated from nonencapsulated free drug via size-exclusion chromatography with Sepharose CL-4B (Sigma Aldrich).

For imaging experiments, identical ghost (no minocycline) formulations were "spiked" with 1,2-dioleoyl-sn-glycero-3-phosphoethanolamine-*N*-(lissamine rhodamine B sulfonyl). For fluorescent resonance energy transfer (FRET) experiments, similar formulations were engineered that were "spiked" with FRET lipid pairs. Specifically, we utilized (1,2-dipalmitoyl-*sn*-glycero-3-phosphoethylthio)-3′'-succinimide)-*N*-(3′-Fluoranthyl) (DSP-F), which exhibits an excitation of 365 nm and an emission of 465 nm, and 1-oleoyl-2-[6-{(7-nitro-2-1,3-benzoxadiazol-4-yl)amino}hexanoyl]-sn-glycero-3-phosphoethanolamine (PS-NBD), which has an excitation of 465 nm and an emission of 534 nm. Controls for the FRET liposomes were nanoliposomes that contain only one of the fluoroprobes in the FRET pair. To differentiate FRET liposomes from control liposomes, we excited the liposome at 365 nm and visualized emission at 534 nm. The phenomenon of FRET was used to determine if liposomes are transported to the retina in an intact state. If disassembled, the liposomal components would not be detectable by FRET. In all experiments, fluorescent lipids were added so that they constituted less than 0.5% of the total lipids as measured by molar percentage.

Liposomal evaluation

The size (nanometers) and zeta potential (millivolts) of newly synthesized minocycline nanoliposomal formulations were evaluated over time using a Malvern Dynamic Light Scattering instrument (Malvern Instruments, Southborough, Massachusetts). Briefly, liposomes recently purified from a CL-4B column were then diluted 10-fold and placed into a cuvette and observed using quasi elastic light scattering. To evaluate the mass of minocycline encapsulated into nontoxic, anionic, nanoscale liposomes we utilized a MDS/SCIEX 4000 Q-Trap mass spectrometer (AB SCIEX, Framingham, Massachusetts) using a C-18 high-pressure liquid chromatography column. The signal intensity of the mass-to-charge ratio detected from the Q-Trap was then compared to a standard curve of minocycline concentrations to allow extrapolation of the quantity of minocycline present in the sample.

STZ-induced diabetic model

All rats were maintained under specific pathogen-free conditions in compliance with protocols approved by the Institutional Animal Care and Use Committee of Penn State College of Medicine, and monitored by quarterly sentinel testing. Male Sprague Dawley rats (Charles River Laboratories, Wilmington, Massachusetts) were purchased at 200–225 g. Experimental type I diabetes was induced after 7 days of acclimation and an overnight fast, with an intraperitoneal injection of 65 mg/kg STZ (Sigma Aldrich) in 10 mM sodium citrate, pH 4.5 (vehicle). Rats that did not receive STZ served as nondiabetic age-matched controls for selected studies. These nondiabetic animals were intraperitoneally administered a comparable volume of vehicle only. Food and water were available to all rats ad libitum, and they were housed under a 12-hour light/dark cycle. Body weights and blood glucose levels were first monitored 7 days post induction and once a week thereafter. At no time throughout the experiment was exogenous insulin administered to attain glycemic control. Glycemic levels of control rats were 122.0 ± 8.4 mg/dL, and diabetic rats' levels averaged 495.0 ± 17.6 mg/dL throughout the experiment. Twelve weeks after diabetic induction, rats were given 20 μL, 10 μL, and 5 μL of subconjunctival, topical, and intravitreal volumes, respectively, of the various treatments once a day for 4 days. To aid in the administration of the subconjunctival injections, the rats were briefly sedated with the use of a gas mixture consisting of 70% CO_2–30% O_2. The rats were placed in a Plexiglas box, then flooded with

the gas mixture and allowed to breathe the gas for no more than 1.5 minutes. After this exposure to the 70% CO_2–30% O_2, the rats were removed from the box and typically remained anoxiated for 45–60 seconds, allowing drug administration. No signs of distress were observed in rats upon their waking. At the conclusion of the experimental treatment protocol, the rats were given a lethal dosage of sodium pentobarbital (100 mg/kg) via intraperitoneal injection, and retinas were harvested and snap-frozen in liquid nitrogen, or rat eyes were dissected and cornea, lens, vitreous, and retina were isolated. For fluorescent experiments, animals received in their left eye either fluorescently labeled rhodamine liposomes or nonfluorescent (ghost) liposomes. The contralateral (right) eye did not receive any treatment and served as control. For the drug delivery experiments, animals either received liposomes containing minocycline, liposomes devoid of minocycline, free minocycline, or no treatment at all. Minocycline was extracted from the tissue by homogenization in a solution of water, methanol, and formic acid 79:20:1 (v/v/v), and then centrifugation at 14,000 rcf followed by quantifying the supernatant concentration using a MDS/SCIEX 4000 Q-Trap mass spectrometer.

DNA fragmentation analysis

A cell death detection enzyme-linked immunosorbent assay (ELISA) protocol (Roche, Mannheim, Germany) was employed to detect fragmented retinal DNA, indicative of late-stage apoptosis. Briefly, retinas were thawed on ice and then homogenized in 200 μL of the provided lysis buffer and allowed to stand for 30 minutes at room temperature. The lysates were centrifuged for 10 minutes at 500 rcf at room temperature. Into separate wells of the ELISA plate, 20 μL of each sample supernatant were added; then, 80 μL of the provided immunoreagent was added to each well and the microplate covered and incubated at room temperature for 2 hours on an orbital rocker at 300 rpm. The immunoreagent was then removed, and the wells were washed three times with incubation buffer. Then, 100 μL of 2,2′-azino-bis(3-ethylbenzthiazoline-6-sulfonic acid) solution were added to each well and incubated in the same manner for 10–20 minutes. DNA fragmentation was quantified as follows: DNA fragmentation = $(OD_{sample} - OD_{negative\ control})$/retinal weight.

Western blots

Retinas were lysed by sonication in NP-40 lysis buffer (50 mM HEPES, 137 mM NaCl, 2 mM Na_3VO_4, 10 mM sodium pyrophosphate, 1% NP-40, 10% glycerol, 50 mM NaF, 1 mM EGTA, 2 mM EDTA, 2 mM β-glycerophosphate, and protease inhibitors) and total protein content was determined by the D_C protein assay (Bio-Rad, Hercules, California). Lysates were then separated by sodium dodecyl sulfate–polyacrylamide gel electrophoresis and transferred to nitrocellulose. Membranes were incubated with horseradish peroxidase–conjugated secondary antibody. We analyzed the expression of galectin-3, annexin V (Santa Cruz Biotechnology, Santa Cruz, California), STAT3 (Cell Signaling, Danvers, Massachusetts), and β-actin (Sigma-Aldrich). Antigen detection was performed using the Pierce ECL Western Blotting Substrate (Thermo, Waltham, Massachusetts), and protein expression was quantified by densitometric analysis using ImageJ.

qPCR

Quantitative polymerase chain reaction (qPCR) analysis was conducted with the use of a 7900 HT Sequence Detection System (Applied Biosystems, Foster City, California), using a 384-well optical format, with Assay-on-Demand (Applied Biosystems) gene-specific primers and probes. SDS 2.2.2 software using the $2^{-}\Delta^{\Delta Ct}$ analysis method was used to quantitate the differential amounts of product using β-actin as an endogenous control.[27] β-actin messenger RNA (mRNA) transcript expression was found to be statistically equivalent in an absolute quantitation experiment (data not shown). Primer and probe sets have previously been reported.[6] Statistical tests for qPCR data is a one-way analysis of variance

(ANOVA) Kruskal-Wallis test followed by a Dunn's Multiple Comparison test and a standard two-tailed parametric *t*-test with an $\alpha < 0.05$.

Results

Characterization of minocycline-encapsulated nanoliposomes

Quasi elastic light scattering characterized size-excluded nanoliposomes to be unilamellar vesicles with an average diameter of 80 ± 20 nm. Analysis of the zeta potential determined that the nanoliposomes were slightly anionic at −21 mV. The shelf-life stability of minocycline-encapsulated nanoliposomes was determined as a function of time and temperature, and was determined not to change from 1 hour to 2 days or from +4°C to 30°C. Stability was maintained in various biological media including DMEM with or without 5% (v/v) fetal bovine serum. Encapsulation efficiencies of nanoliposomal minocycline formulations were evaluated via mass spectroscopy. A 100 mM stock solution was mixed with lipids before sonication and extrusion for 30 minutes to formulate a 20.3 mM encapsulation buffer. After sonication and size extrusion, this was then purified by CL-4B size-exclusion chromatography to form the purified nanoliposomal fraction with a concentration of minocycline of 451.0 ± 30 μM. Therefore, the final encapsulation efficiency was shown to be approximately 2% to 3% of the starting loading material as determined by mass spectroscopy.

Delivery of the minocycline-encapsulated nanoliposomes to the retina

Confocal analysis of rhodamine-labeled nanoliposomes was utilized to assess ocular localization after (i) intravitreal injection, (ii) subconjunctival injection, and (iii) topical application to Sprague Dawley rats. Fluorescent staining of the inner and outer plexiform layers and the inner and outer segments as well as the pigmented epithelium layer of the retina was visible after 15 minutes of administration for all delivery modalities (Figure 1). A small degree of autofluorescence indicative of frozen retinal sections can be visualized in control sections, but the greater intensity of staining in rhodaminelabeled liposome-treated eyes shows definitive positive staining. Liposomes that did not contain rhodamine and sections from the contralateral eye that did not receive any treatment served as negative controls. Subconjunctival injections had the most intense fluorescence, followed by topical administration, and then intravitreal injections—all after 15 minutes. Similar results were observed after 1 hour for subconjunctival injection and topical administration, with little fluorescence observed for intravitreal injection (data not shown), possibly reflecting more rapid clearance for intravitreal administration.

To validate if intact nanoliposomes reach the retina, we employed a FRET liposome via subconjunctival injections. FRET pairs must remain in close proximity (i.e., as components of an intact liposome) to exhibit FRET staining in vivo. We validated our FRET liposomes in vitro using single fluoroprobes (DSP-F or PS-NBD) and both fluoroprobes combined (DSP-F + PS-NBD) (Figure 2, *E*). When both fluoroprobes were combined, the signal was much more intense than when either fluoroprobe was used alone. As controls in our experimental rat retinas, we administered liposomes containing only the first fluoroprobe DSP-F (Figure 2, *B*), only the second fluoroprobe PS-NBD (Figure 2, *C*), or no fluoroprobe at all (Figure 2, *A*), and compared them to the liposome that contained both DSP-F and PS-NBD (Figure 2, *D*). When retinal segments were excited at 365 nm and imaged at 534 nm, fluorescence was only observed with the FRET pair formulation (Figure 2, *D*). The pattern of fluorescence was similar to what was observed with the rhodamine-spiked liposomal formulation (Figure 1). Taken together, these results indicate that the anionic nanoliposomes remain intact as a consequence of transit to the retina.

To conclusively show that intact nanoliposomes can deliver encapsulated cargo to the retinal segments, we utilized mass spectrometry to assess minocycline mass delivered to ocular tissue as a function of subconjunctival administration. Untreated rats and rats treated with liposomes that did not contain minocycline served as negative controls, while nonencapsulated minocycline served as a positive control for the nanoencapsulated minocycline formulation. Retinas were excised at various time points, and extracted minocycline was quantified via mass spectroscopy as described in Methods (Figure 3). Nanoliposomal minocycline delivery increased the mass of minocycline in the retina at all time points as compared to free (nonliposomal) delivered minocycline. At 1 and 6 hours, an approximate one- and fourfold increase was observed for the subconjunctivally administered minocycline liposome vs. free minocycline. Moreover, given a concentration of encapsulated minocycline of 451.0 μM, nearly 40% of the minocycline is localized within the retina 6 hours after subconjunctival administration. Significant cornea localization was also noted, with little localization in the vitreous or the lens. At 24 hours after administration, minocycline has largely been cleared from the retina, but trace amounts near the detection limit of our mass spectrometer still point to localization within the retina.

In vivo toxicity of minocycline liposomes in control rats

We next evaluated the toxicity of nanoliposomal minocycline as a function of a subconjunctival injection administered once daily for 4 days. Fragmented DNA, a marker of apoptosis, was utilized to assess retinal toxicity of nanoliposomal minocycline formulations purified via size-exclusion chromatography (Figure 4). Concentrations of encapsulated minocycline (316 and 31.6 μM) were chosen consistent with the retinal delivery experiments (451 μM). A 10 mM mixture of free and nanoliposomal minocycline that did not undergo CL-4B sizeexclusion chromatography was utilized as a positive control for toxicity. The purified nanoliposomes did not exhibit toxicology as assessed by retinal DNA fragmentation at either of the two pharmacological doses.

Targeted transcriptomic and proteomic biomarker panels can be used as a measure of pharmacological effects

We initially evaluated the efficacy of minocycline-encapsulated nanoliposomes by utilizing a transcriptomic biomarker panel as a surrogate end point for therapeutic efficacy.[6,7] This targeted transcriptomic panel was selected as the minimal number of mRNA transcripts that could be used to define and evaluate DR.[6,7] We analyzed extracts of mRNA from retinal tissue of 3-month-diabetic or control rats injected subconjunctivally once a day for 4 days with vehicle, or with free or encapsulated (316 μM) minocycline. The relative expression of 7 of the 14 gene products was changed by free minocycline administration, returning them to nondiabetic levels (Figure 5). These gene products (Lama5, Gbp2, Chi3l1, Icam1, C1s, C1inh, and Carhsp1) are all associated with proinflammatory phenotypes.[6,7] In contrast, nanoliposomal minocycline failed to produce such a statistically significant change in all but 2 out of the 14 gene targets analyzed (Lama5 and Icam1).

Further analysis of individual animals by support vector machine classification analysis[28] revealed that both free and nanoliposomal minocycline can reverse the transcriptomic biomarker panel in individual rats. This unbiased approach determined that three of the eight animals in the group treated with free minocycline and two of the eight in the group treated with nanoliposomal minocycline exhibited a normal nondiabetic transcript phenotype (Figure 6).

Gene analysis at the transcript level was followed up by analysis of protein expression. We again utilized a targeted biomarker approach, performing western blot analysis on a series of gene products that did not respond to insulin in a previous proteomic screen.[8] Protein levels

of galectin-3 (Lgals3), STAT3, and annexin V have been shown to be upregulated in diabetic animals, yet insulin therapy does not significantly rescue this effect.[8] We found that both free and nanoliposomal minocycline were able to return STAT3 to prediabetic levels (Figure 7). In addition, free minocycline caused galectin-3 to return to prediabetic levels, and liposomal minocycline caused annexin V to return to prediabetic levels. (Figure 7). STAT3 and galectin-3 are inflammatory in the retina,[29,30] and annexin V has been shown to conduct calcium ions.[31] It should be emphasized that these elevated gene products that are downregulated by minocycline were resistant to insulin treatment.[8] Taken together, these transcriptomic and proteomic data suggest that subconjunctivally administered minocycline may have efficacy in diabetic retinopathy models, and, more importantly, document the utility of biomarker panels for ocular therapeutic drug studies.

Discussion

The goal of this study was to elucidate whether local administration of nanoliposomal or free minocycline can deliver a pharmacologically relevant dose of a drug to the retina via local injection. Although it would be preferable to self-administer eye drops to a patient, we chose to focus these proof-of-concept studies to subconjunctival administration in an effort to reduce variability of administration via topical administration. It is also of interest that we observed increased fluorescent imaging with subconjunctival injection compared to intravitreal or topical administration (Figure 2). Thus, we chose to focus the delivery, toxicology, and efficacy studies of minocycline nanoliposomes to subconjunctival-injection protocols.

The unique aspect of the present approach is documentation of encapsulation of a therapeutic dose of minocycline within nontoxic, fusigenic, anionic, nanoscale liposomes that can be used for ocular delivery to posterior segments of the eye. Even though minocycline has been encapsulated in liposomal formulations before[24,32,33] for nonocular uses, our formulation is unique in that size-exclusion chromatography and size extrusion were utilized to generate a nanoliposome devoid of surface minocycline contamination. In fact, without “cleanup” these formulations were toxic (Figure 4). Moreover, shortly after a subconjunctival injection, minocycline nanoliposomes can be effectively trafficked intact to the retina and deliver minocycline in higher, more sustained amounts than when free minocycline is given alone. This ability to remain intact during trafficking is a novel aspect of the formulation and possibly is responsible for the higher concentration of encapsulated minocycline delivered to the retinas compared to free minocycline. We also demonstrate that subconjunctival injections of either nanoliposomal minocycline or free minocycline can reverse a portion of the aberrant expression seen in mRNA or protein-gene profiles documented in STZ-induced diabetic rat retinas. Explanations for the lack of an enhanced effect on the gene panel with minocycline-encapsulated nanoliposomes compared with free minocycline, despite the improved kinetic delivery, might reflect nonoptimized minocycline dosage and duration of treatment protocols. Alternatively, this lack of efficacy for liposomal minocycline to reduce all of the inflammatory transcriptomic biomarkers on the panel, in comparison to free minocycline, may reflect liposomal trafficking of minocycline to lysosomes, where it is degraded. The use of less fusigenic liposomal formulations (i.e., less cholesterol) could remedy this putative liposomal trafficking. However, that both free minocycline and nanoliposomal minocycline demonstrated a positive impact on select “proinflammatory” end points suggests efficacy after local delivery, which could potentially improve with an optimization of dosage and duration of treatment.

Many drugs that have potential therapeutic utility in DR are ultimately limited because of adverse outcomes on other systems when the drug is given systemically.[20-22] In order to treat the retina with a systemic treatment regimen of minocycline, the blood plasma levels of

the drug would have to be very high over long periods of time. This may needlessly expose the entire body to high doses of the drug and increase the chance of adverse reactions. This is especially problematic for minocycline, in that an adverse side effect of systemic high-dose therapy for teenage acne is pharmacological induction of lupus. Subconjunctival local administration of nanoliposomal minocycline can potentially be used to administer these high therapeutic doses to the retina without inducing systemic toxicities. In fact, clearance mechanisms, by definition, would dilute the minocycline concentration as it diffuses into the systemic circulation. In fact, we believe that the concentration measured in the retina by mass spectrometry (~2 μM at 6 hours) could not be achieved after systemic dilution. In addition, ocular delivery of nanoliposomal minocycline can potentially reduce or delay clearance mechanisms within the eye. Finally, nanoliposomal or free minocycline can be administered directly to the site of action and thus avoid first-pass metabolism as well as side effects involving depletion of normal flora in the gut. Taken together, the engineering of a nontoxic nanoliposomal formulation that remains intact during ocular delivery has the potential to deliver therapeutic doses of anti-inflammatory agents to combat diseases such as DR.

Acknowledgments

The authors would like to acknowledge the contribution of Wendy Dunton to this work for her exceptional handling of the animals during drug administration and tissue collection.

This work was supported by the Juvenile Diabetes Research Foundation (JDRF) Diabetic Retinopathy Center (4-2002-455 to M.K. and T.W.G.); a JDRF postdoctoral fellowship (to T.E.F.); Pennsylvania Tobacco Settlement Funds (to W.F.); L01 EY021716 (to W.F.), R01 EY18336-02 (to M.K.), and EY020582 (to T.W.G.) from the National Eye Institute; and the American Diabetes Association.

References

1. Schwartz SG, Flynn HW Jr. Pharmacotherapies for diabetic retinopathy: present and future. Exp Diabetes Res. 2007; 2007:52487. [PubMed: 17713597]
2. Sahoo SK, Dilnawaz F, Krishnakumar S. Nanotechnology in ocular drug delivery. Drug Discov Today. 2008; 13:144–51. [PubMed: 18275912]
3. Short BG. Safety evaluation of ocular drug delivery formulations: techniques and practical considerations. Toxicol Pathol. 2008; 36:49–62. [PubMed: 18337221]
4. Ghate D, Edelhauser HF. Ocular drug delivery. Expert Opin Drug Deliv. 2006; 3:275–87. [PubMed: 16506953]
5. Antonetti DA, Barber AJ, Bronson SK, Freeman WM, Gardner TW, Jefferson LS, et al. JDRF Diabetic Retinopathy Center Group. Diabetic retinopathy: seeing beyond glucose-induced microvascular disease. Diabetes. 2006; 55:2401–11. [PubMed: 16936187]
6. Brucklacher RM, Patel KM, VanGuilder HD, Bixler GV, Barber AJ, Antonetti DA, et al. Whole genome assessment of the retinal response to diabetes reveals a progressive neurovascular inflammatory response. BMC Med Genomics. 2008; 13:26. [PubMed: 18554398]
7. Freeman WM, Bixler GV, Brucklacher RM, Lin CM, Patel KM, VanGuilder HD, et al. A multistep validation process of biomarkers for preclinical drug development. Pharmacogenomics J. 2010; 10:385–95. [PubMed: 19997081]
8. van Guilder HD, Bixler GV, Kutzler L, Brucklacher RM, Bronson SK, Kimball SR, et al. Multi-modal proteomic analysis of retinal protein expression alterations in a rat model of diabetic retinopathy. PLoS One. 2011; 6:e16271. [PubMed: 21249158]
9. Brundula V, Rewcastle NB, Metz LM, Bernard CC, Yong VW. Targeting leukocyte MMPs and transmigration: minocycline as a potential therapy for multiple sclerosis. Brain. 2002; 125(Pt 6): 1297–308. [PubMed: 12023318]
10. Sutton TA, Kelly KJ, Mang HE, Plotkin Z, Sandoval RM, Dagher PC. Minocycline reduces renal microvascular leakage in a rat model of ischemic renal injury. Am J Physiol Renal Physiol. 2005; 288:F91–7. [PubMed: 15353401]

11. Yao JS, Chen Y, Zhai W, Xu K, Young WL, Yang GY. Minocycline exerts multiple inhibitory effects on vascular endothelial growth factor–induced smooth muscle cell migration: the role of ERK1/2, PI3K, and matrix metalloproteinases. Circ Res. 2004; 95:364–71. [PubMed: 15256478]
12. Chu LS, Fang SH, Zhou Y, Yin YJ, Chen WY, Li JH, et al. Minocycline inhibits 5-lipoxygenase expression and accelerates functional recovery in chronic phase of focal cerebral ischemia in rats. Life Sci. 2010; 86:170–7. [PubMed: 20006627]
13. Song Y, Wei EQ, Zhang WP, Ge QF, Liu JR, Wang ML, et al. Minocycline protects PC12 cells against NMDA-induced injury via inhibiting 5-lipoxygenase activation. Brain Res. 2006; 1085:57–67. [PubMed: 16574083]
14. Heo K, Cho YJ, Cho KJ, Kim HW, Kim HJ, Shin HY, et al. Minocycline inhibits caspase-dependent and -independent cell death pathways and is neuroprotective against hippocampal damage after treatment with kainic acid in mice. Neurosci Lett. 2006; 398:195–200. [PubMed: 16469440]
15. Matsuki S, Iuchi Y, Ikeda Y, Sasagawa I, Tomita Y, Fujii J. Suppression of cytochrome c release and apoptosis in testes with heat stress by minocycline. Biochem Biophys Res Commun. 2003; 312:843–9. [PubMed: 14680842]
16. Vincent JA, Mohr S. Inhibition of caspase-1/interleukin-1beta signaling prevents degeneration of retinal capillaries in diabetes and galactosemia. Diabetes. 2007; 56:224–30. [PubMed: 17192486]
17. Steinmeyer J, Daufeldt S, Taiwo YO. Pharmacological effect of tetracyclines on proteoglycanases from interleukin-1-treated articular cartilage. Biochem Pharmacol. 1998; 55:93–100. [PubMed: 9413935]
18. Chen M, Ona VO, Li M, Ferrante RJ, Fink KB, Zhu S, et al. Minocycline inhibits caspase-1 and caspase-3 expression and delays mortality in a transgenic mouse model of Huntington disease. Nat Med. 2000; 6:797–801. [PubMed: 10888929]
19. Krady JK, Basu A, Allen CM, Xu Y, LaNoue KF, Gardner TW, et al. Minocycline reduces proinflammatory cytokine expression, microglial activation, and caspase-3 activation in a rodent model of diabetic retinopathy. Diabetes. 2005; 54:1559–65. [PubMed: 15855346]
20. Angulo JM, Sigal LH, Espinoza LR. Coexistent minocycline-induced systemic lupus erythematosus and autoimmune hepatitis. Semin Arthritis Rheum. 1998; 28:187–92. [PubMed: 9872479]
21. Losanoff JE, Holder-Murray JM, Ahmed EB, Cochrane AB, Testa G, Millis JM. Minocycline toxicity requiring liver transplant. Dig Dis Sci. 2007; 52:3242–4. [PubMed: 17404879]
22. Somech R, Arav-Boger R, Assia A, Spirer Z, Jurgenson U. Complications of minocycline therapy for acne vulgaris: case reports and review of the literature. Pediatr Dermatol. 1999; 16:469–72. [PubMed: 10632948]
23. Schrodt BJ, Callen JP. Polyarteritis nodosa attributable to minocycline treatment for acne vulgaris. Pediatrics. 1999; 103:503–4. [PubMed: 9925852]
24. Sangare L, Morisset R, Omri A, Ravaoarinoro M. Incorporation rates, stabilities, cytotoxicities and release of liposomal tetracycline and doxycycline in human serum. J Antimicrob Chemother. 1998; 42:831–4. [PubMed: 10052911]
25. Sangare L, Morisset R, Ravaoarinoro M. In-vitro anti-chlamydial activities of free and liposomal tetracycline and doxycycline. J Med Microbiol. 1999; 48:689–93. [PubMed: 10403420]
26. Stover TC, Sharma A, Robertson GP, Kester M. Systemic delivery of liposomal short-chain ceramide limits solid tumor growth in murine models of breast adenocarcinoma. Clin Cancer Res. 2005; 11:3465–74. [PubMed: 15867249]
27. Livak KJ, Schmittgen TD. Analysis of relative gene expression data using real-time quantitative PCR and the 2(-delta delta C(T)) method. Methods. 2001; 25:402–8. [PubMed: 11846609]
28. Mitchell RM, Freeman WM, Randazzo WT, Stephens HE, Beard JL, Simmons Z, et al. A CSF biomarker panel for identification of patients with amyotrophic lateral sclerosis. Neurology. 2009; 72:14–9. [PubMed: 18987350]
29. Ozawa Y, Nakao K, Kurihara T, Shimazaki T, Shimmura S, Ishida S, et al. Roles of STAT3/SOCS3 pathway in regulating the visual function and ubiquitin-proteasome-dependent degradation of rhodopsin during retinal inflammation. J Biol Chem. 2008; 283:24561–70. [PubMed: 18614536]

30. Rabinovich GA, Liu FT, Hirashima M, Anderson A. An emerging role for galectins in tuning the immune response: lessons from experimental models of inflammatory disease, autoimmunity and cancer. Scand J Immunol. 2007; 66:143–58. [PubMed: 17635792]

31. Berendes R, Voges D, Demange P, Huber R, Burger A. Structure-function analysis of the ion channel selectivity filter in human annexin V. Science. 1993; 262:427–30. [PubMed: 7692599]

32. Hu W, Metselaar J, Ben LH, Cravens PD, Singh MP, Frohman EM, et al. PEG minocycline-liposomes ameliorate CNS autoimmune disease. PLoS One. 2009; 4:e4151. [PubMed: 19127301]

33. Sangare L, Morisset R, Ravaoarinoro M. In vitro inhibition of chlamydia trachomatis growth by liposome-encapsulated cyclines. Pathol Biol (Paris). 2001; 49:53–6. [PubMed: 11265224]

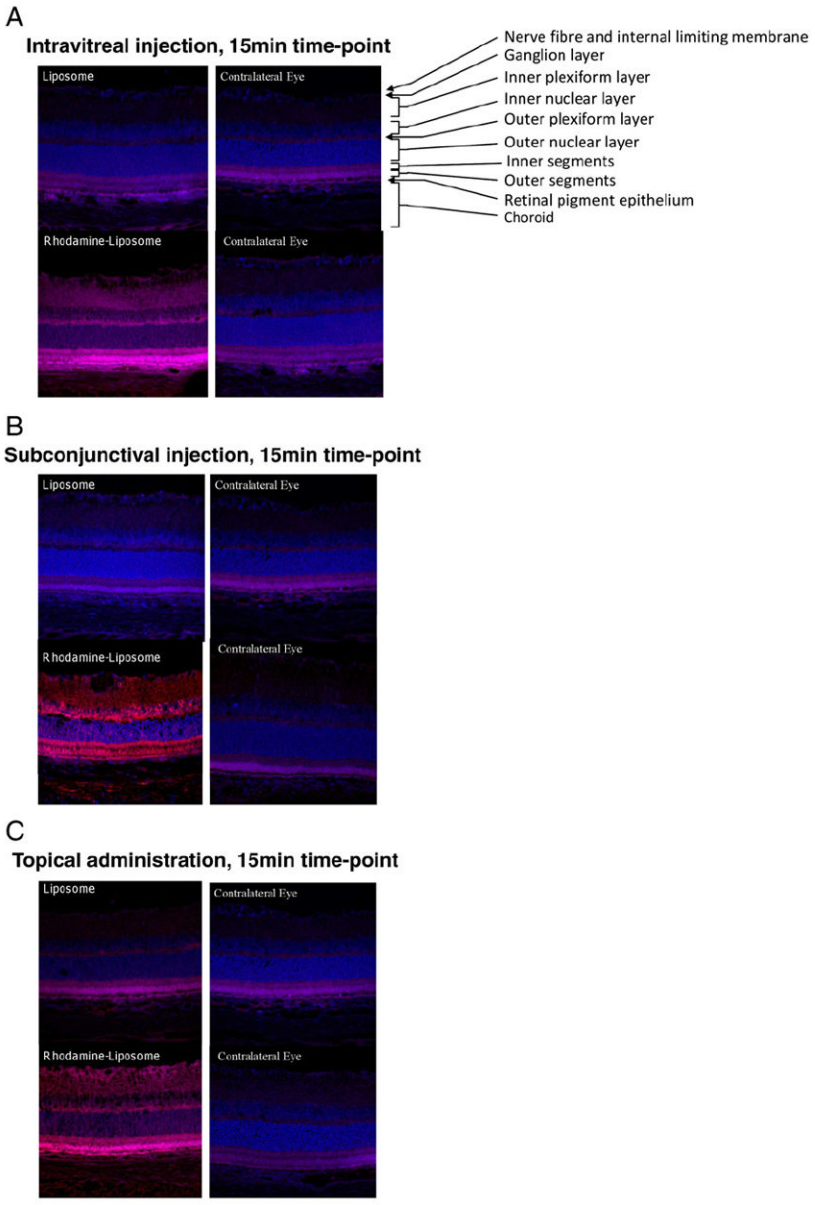

Figure 1.

Rhodamine-labeled liposomes image the retina 15 minutes after administration via different methods. Retinal sections 10 μm thick were used for imaging. Shown are representative photomicrographs from **(A)** intravitreal injection, **(B)** subconjunctival, and **(C)** topical administration methods. In each panel, the eyes from two animals are depicted. The top left section, corresponding to the left eye of the first animal, was treated with nonfluorescent (ghost) liposomes, and the bottom left section, corresponding to the left eye of the second animal, was treated with liposomes labeled with rhodamine. The contralateral (right) eyes of both animals are depicted on the right-hand side of the panels. In these photomicrographs, DAPI-stained nuclei (blue) and rhodamine-labeled nanoliposomes (*red*) are shown. The various layers of the retina are labeled in the top right section of panel **A**.

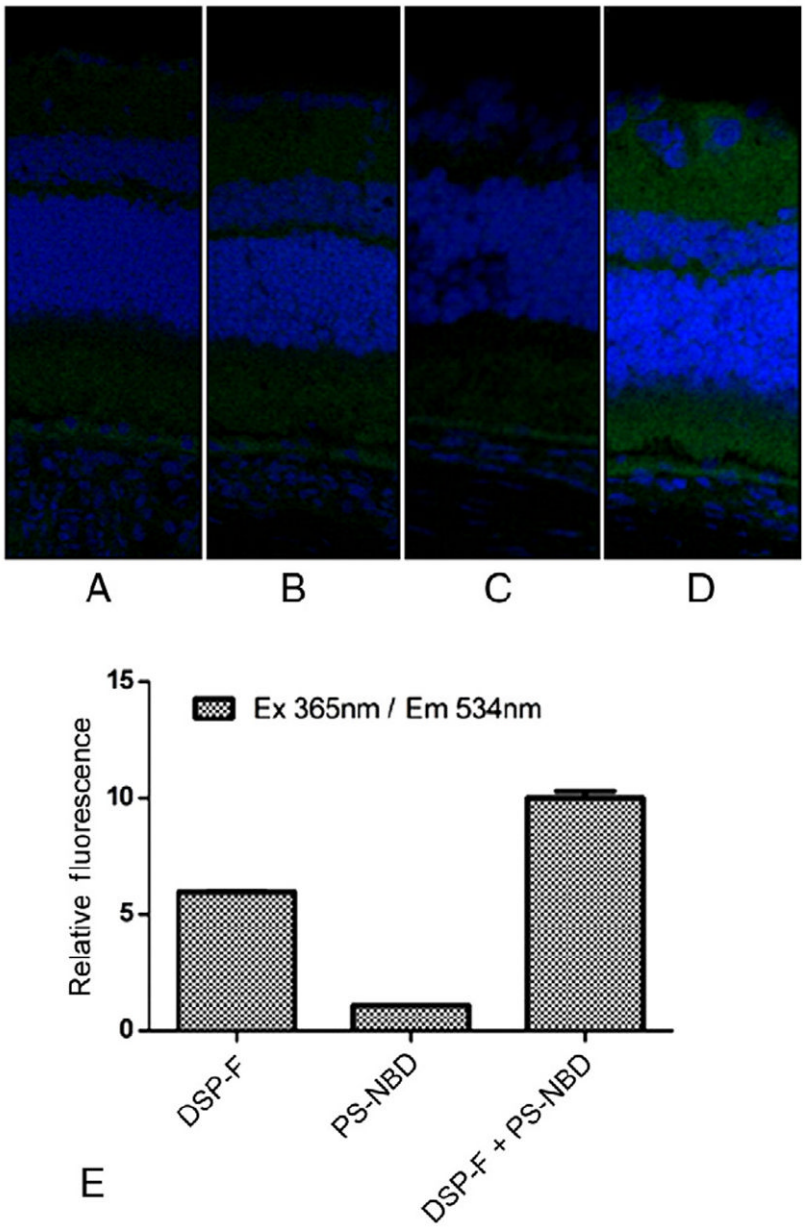

Figure 2.

Sprague Dawley rats were administered 20-μL subconjunctival injections with fluorescence resonance energy transfer (FRET) nanoliposomes or appropriate controls. After 15 minutes, retinas were extracted and prepared for frozen sectioning. FRET was assessed by exciting at 365 nm (DSP-F) and observing emissions at 534 nm (PS-NBD). **(A)** Nanoliposomes containing no fluoroprobe. **(B)** Nanoliposomes containing only DSP-F. **(C)** Nanoliposomes containing only PS-NBD. **(D)** Nanoliposomes containing both DSP-F and PS-NBD. Albeit the change in retinal staining is subtle, the signal seen in panel D treated with the complete FRET liposome displays a fluorescent signal that is brighter than background autofluorescence seen in panels **A, B**, and **C. (E)** Validation of the FRET assay. When excited at 365 nm and detected at 534 nm, DSP-F + PS-NBD gave a greater signal than DSP-F or PS-NBD alone.

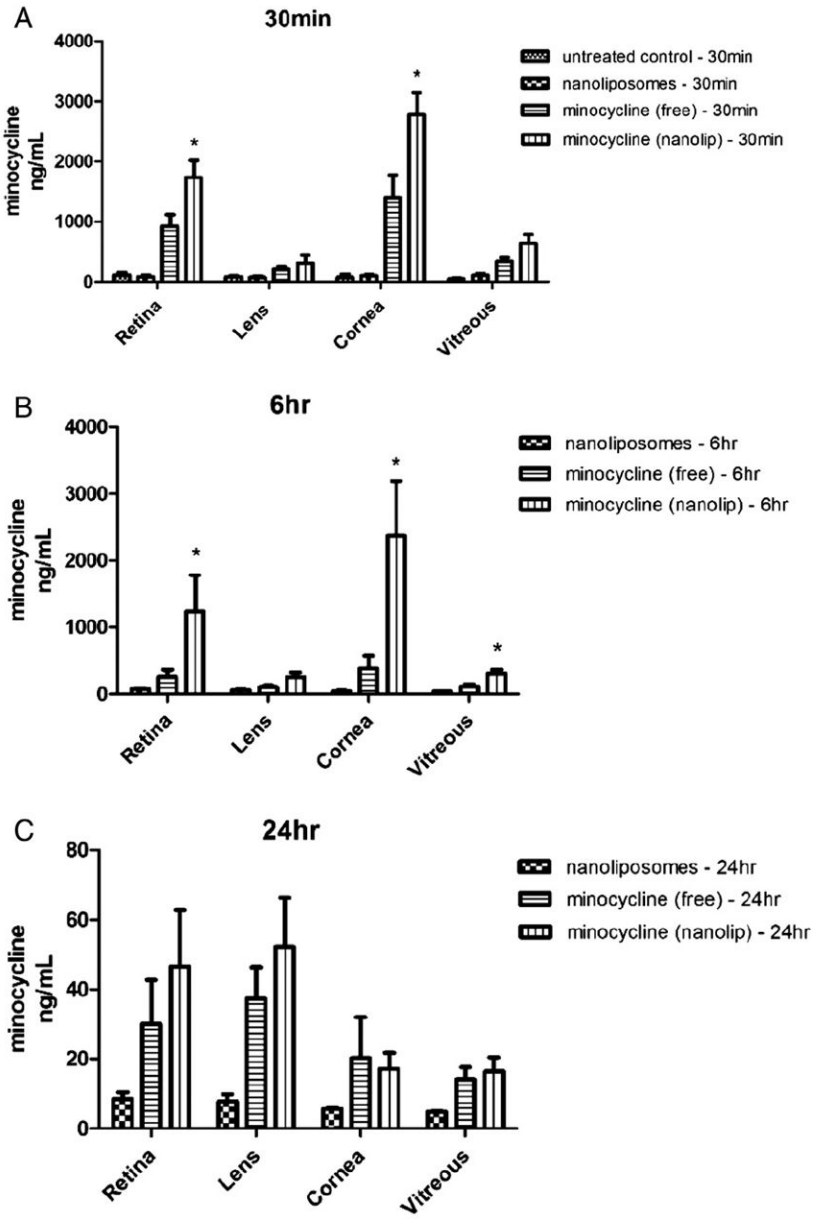

Figure 3.

Nanoliposomal encapsulation increases the concentration of minocycline in various tissues of the eye. Elevated mass levels of minocycline are detected at **(A)** 30 minutes and **(B)** 6 hours after subconjunctival administration of nanoliposomal minocycline compared with nonliposomal (free) minocycline or ghost (no minocycline) liposomes. Note the changed *y*-axis scale in panel **C**, reflecting clearance from ocular tissues at 24 hours. Asterisk denotes statistical significance between the marked column and the same tissue treated with free minocycline alone, as determined by a one-tailed nonparametric Mann-Whitney *t*-test (*α = 0.05).

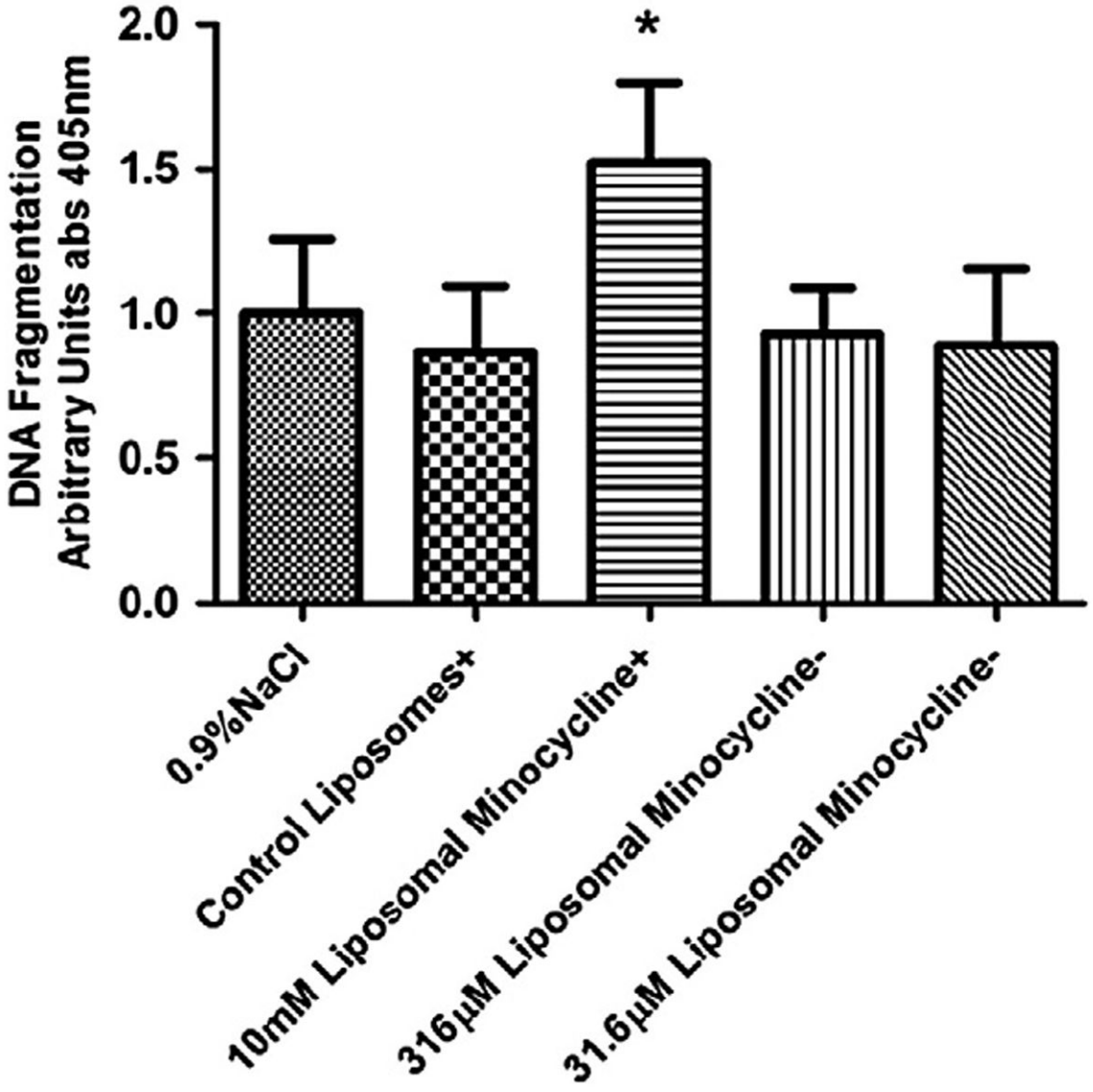

Figure 4.

Level of fragmented DNA found in rat retinal lysates as detected with the Roche Cell Death Detection enzyme-linked immunosorbent assay. There was no increase in fragmented DNA detected when the animals were treated only with control nanoliposomes or nanoliposomal minocycline at concentrations of 316 μM or 31.6 μM minocycline as compared to animals treated with 0.9% NaCl irrigation fluid. The control and the 10 mM minocycline treatments were not exposed to CL-4B size-exclusion chromatography that removes surface-contaminated minocycline (+). In previous experiments (data not shown), this 10 mM free/nanoliposomal minocycline preparation was observed to induce apoptosis and here serves as a positive control. However, the equivalent preparation of liposomes without minocycline causes no such increase in DNA cleavage at this concentration and with this treatment regimen. 316 μM and 31.6 μM nanoliposomal minocycline preparations were purified via CL-4B size-exclusion chromatography (−). This step eliminates nonencapsulated minocycline and greatly reduces the concentration of minocycline in the preparation. In this experiment, increases in DNA cleavage were not detected in rat retinal lysates from rats treated with these preparations. Asterisk denotes statistical significance between the marked

column and the retinal samples treated with 0.9% NaCl irrigation fluid as determined by a one-tailed nonparametric Mann-Whitney *t*-test (*$\alpha = 0.05$).

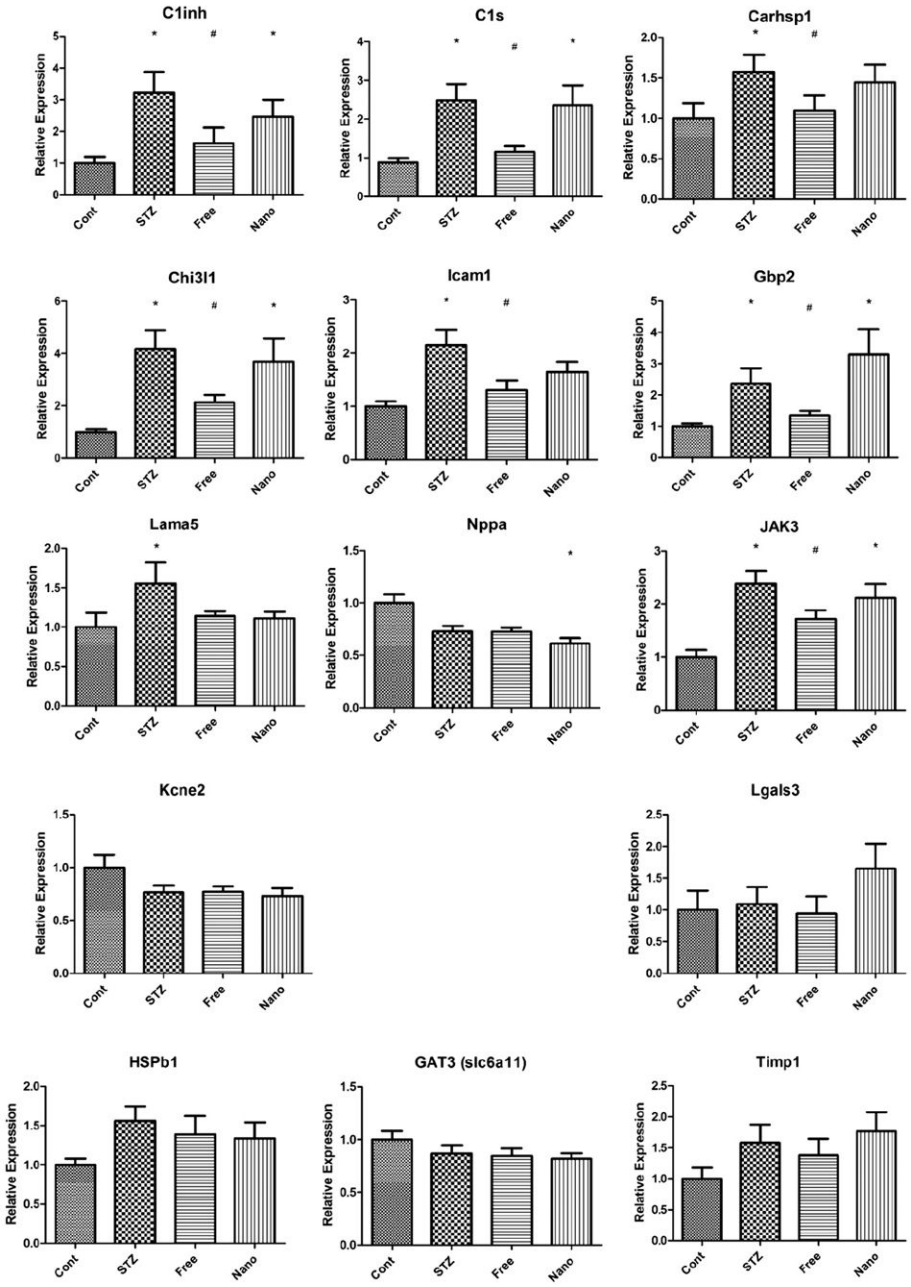

Figure 5.

Relative expression of the minimal number of mRNA transcripts that would allow differentiation of diabetic from control individuals as determined by Freeman et al.[7] We utilized this transcriptomic panel to assess free and nanoliposomal minocycline subconjunctival treatment in normal and STZ-treated animals after 3 months. Both nanoliposomal minocycline-treated and free minocycline-treated groups were treated with the subconjunctivally administered 20 μL of 316 μM minocycline once a day for 4 days after the 3 months of STZ-induced diabetes. Asterisks denote transcripts having significantly different means as determined by a Kruskal-Wallis one-way ANOVA, where the asterisks appear over the groups that were determined to differ significantly from the control group as determined by Dunn's post test (*$P < 0.1$). Number signs denote the free minocycline-

treated groups that were found to differ significantly from the STZ group, as determined by a one-tailed Mann-Whitney *t*-test ($^{\#}P < 0.05$). The first nine genes changed significantly, while the last five did not.

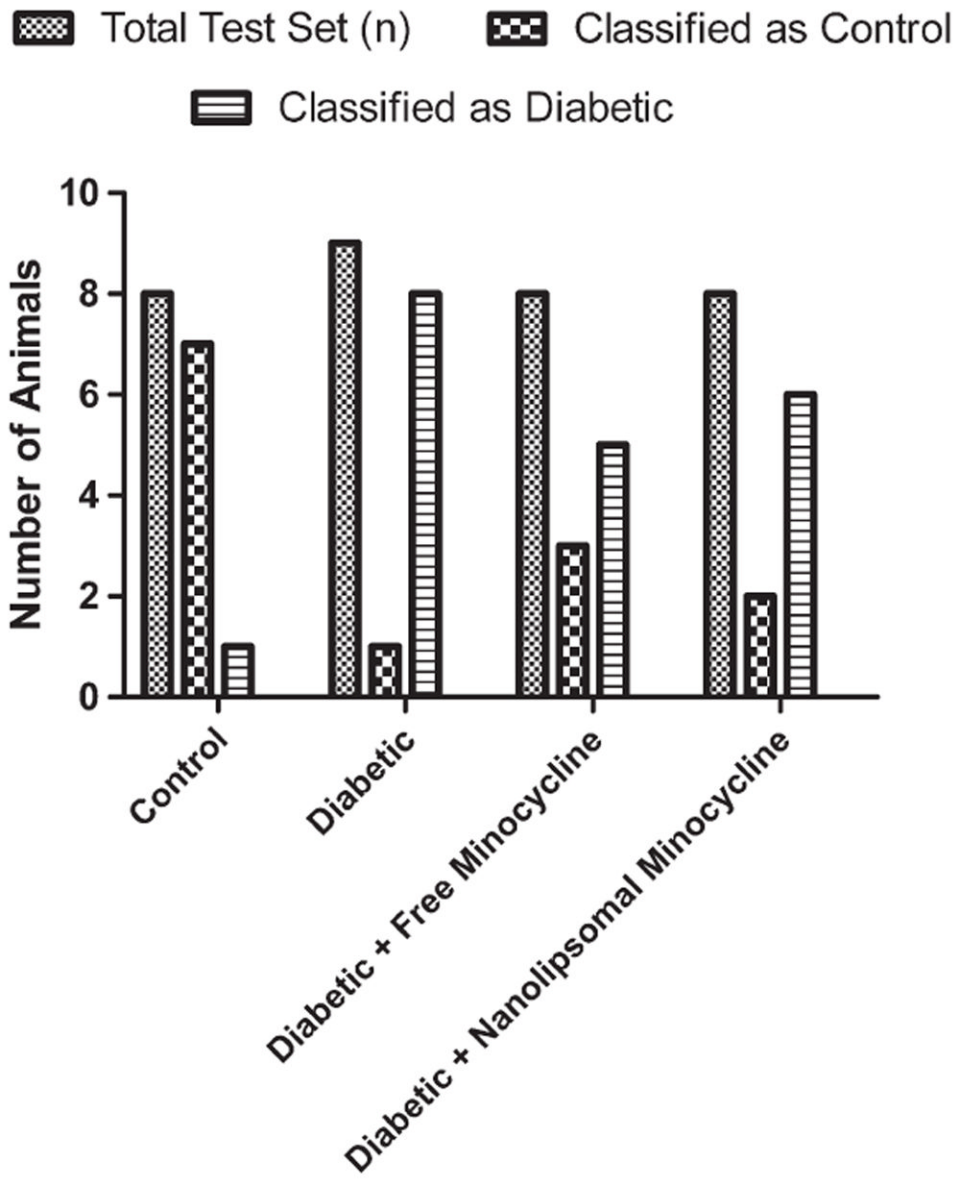

Figure 6.

Support vector machine classification analysis with polynomial kernel scale factor of 1. Both nanoliposomal minocycline-treated and free minocycline-treated groups were treated with 20 μL of subconjunctivally administered minocycline at a concentration of 316 μMonce a day for 4 days after 3 months of STZ-induced diabetes.

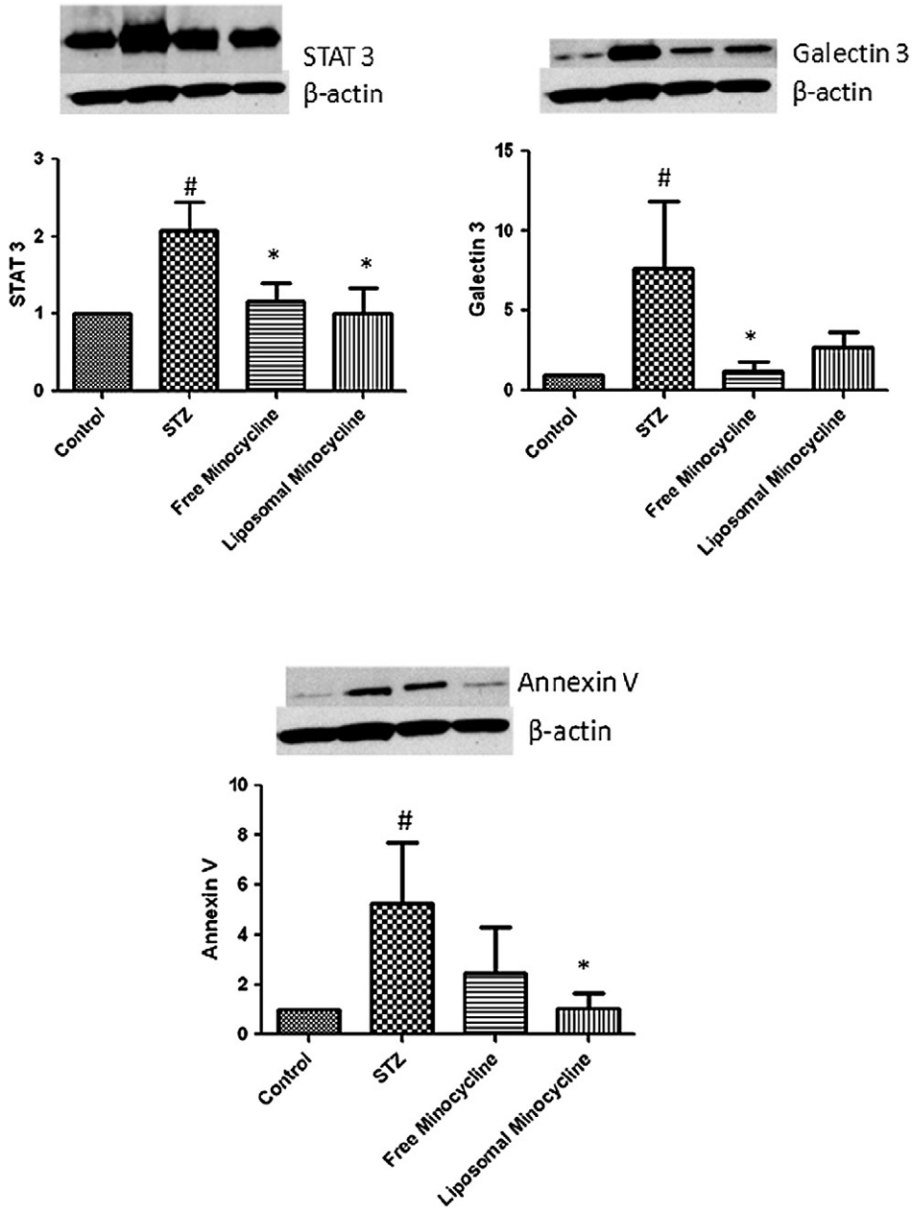

Figure 7.

Relative protein levels of genes previously described by van Guilder et al[8] to be differentially expressed in STZ-induced diabetic rats that were unaffected by intensive insulin treatment. Western blots and corresponding histograms are shown. For each protein, the relative expression was determined in free minocycline-treated and nanoliposomal minocycline-treated 3-month-old rats. Both nanoliposomal minocycline-treated and free minocycline-treated groups were treated with 20 μL of 316 μM minocycline subconjunctivally administered once a day for 4 days after 3 months of STZ-induced diabetes. See text for details. Number signs denote protein levels with significantly different means compared to the control group using a one-tailed Student's *t*-test ($^{\#}P < 0.1$). Asterisks denote protein levels with significantly different means compared to the STZ group using a one-tailed Student's *t*-test ($^{*}P < 0.1$).